Available online at www.sciencedirect.com
ScienceDirect
C. R. Geoscience 341 (2009) 473–485
COMPTES RENDUS GEOSCIENCE

Surface geosciences (Hydrology–Hydrogeology)

Monitoring of water and heat transfer in the vadose zone of a carbonate formation: An example of an underground quarry in Gironde, France

Adrian Cerepi *, Corinne Loisy, René Burlot

EA GHYMAC 4134, institut EGID Bordeaux-3, université de Bordeaux, 1, allée F.-Daguin, 33607 Pessac cedex, France

Received 24 August 2007; accepted after revision 23 March 2009
Available online 11 June 2009

Presented by Ghislain de Marsily

Abstract

This article studies the water and heat transfer in the vadose zone of a carbonate formation during three hydrological cycles (August 2001–May 2004). The application of the time domain reflectometry (TDR) method to determine the volumetric water content of porous rocks has been widely investigated. The study of more than 285 monthly point measurements of the rock water content during three hydrological cycles, distributed throughout an abandoned underground quarry in Gironde, France, shows a permanently undersaturated limestone (between 35% and 50%). Three periods of maximum volumetric water content correspond to the occurrence of three effective rainfall events. The phase lag and amplitude damping of the hydraulic and thermal signals with depth can be modelled and explained by the hydraulic and thermal properties of the porous medium in the unsaturated zone. ***To cite this article: A. Cerepi et al., C. R. Geoscience 341 (2009).***

Résumé

Étude expérimentale des transferts hydriques et thermiques dans la zone vadose d'une formation réservoir carbonatée : exemple d'une carrière souterraine en Gironde, France. Cet article a pour objectif l'étude expérimentale, in situ, des transferts d'eau et de chaleur, dans la zone vadose, dans le cas des formations sédimentaires carbonates, durant trois cycles hydrologiques (août 2001–mai 2004). La méthode de la réflectométrie en domaine temporel (TDR) a été utilisée pour déterminer la teneur en eau du massif poreux. Plus de 285 points de mesure de teneur en eau réalisés mensuellement durant trois cycles hydrologiques, répartis dans une carrière souterraine abandonnée en Gironde, France, montrent une variation de la saturation du calcaire entre 35 % et 50 %. Les trois périodes de maximum de teneur en eau correspondent à trois événements de précipitations efficaces importants. Le déphasage et l'atténuation des signaux hydriques et thermiques avec la profondeur sont modélisés et expliqués par les propriétés hydraulique et thermique du milieu poreux dans la zone vadose. ***Pour citer cet article : A. Cerepi et al., C. R. Geoscience 341 (2009).***

Keywords: Vadose zone; Limestone; Porous medium; Underground quarry; Water content; Thermal transfer

Mots clés : Zone vadose ; Calcaire ; Milieu poreux ; Carrière souterraine ; Teneur en eau ; Transfert thermique

* Corresponding author.
E-mail address: adrian.cerepi@egid.u-bordeaux3.fr (A. Cerepi).

1631-0713/$ – see front matter
doi:10.1016/j.crte.2009.03.007

Nomenclature

$A(z)$	amplitude of signals at depth $\|z\|$
$A(0)$	amplitude of the input signal
C_o	velocity of light (m s^{-1})
C	velocity of an electromagnetic wave (m s^{-1})
C_s	volumetric heat capacity of the solid fraction (J m^3 K^{-1})
C_v	volumetric heat capacity of medium (J m^3 K^{-1})
C_w	volumetric heat capacity of water (J m^3 K^{-1})
D_h	hydraulic diffusivity (m s^{-1})
D_{th}	thermal diffusivity (m^2 s^{-1})
ET_r	real evapotranspiration
k	saturated hydraulic conductivity (m s^{-1})
k_n	thermal conductivity of an unsaturated medium (W m^{-1} K^{-1})
k_s	thermal conductivity of the solid fraction (W m^{-1} K^{-1})
k_{eff}	effective hydraulic conductivity (m s^{-1})
k_{rw}	relative water permeability
K^*	complex dielectric constant
K'	real part of the dielectric constant
K''	imaginary part of the dielectric constant
P_b	bubling pressure (Pa)
P_c	capillary pressure (Pa)
P_{eff}	effective rainfall
R	coefficient of spatial representativity of measurements
t_h	phase lag of hydric transfer from the modelling (s)
t'_h	hydric phase lag observed (s)
t_{th}	phase lag of thermal transfer from the modelling (s)
t'_{th}	thermal phase lag observed (s)
Ta	desaturation rate (% $days^{-1}$)
Tr	saturation rate (% $days^{-1}$)
S_e	the normalized saturation
S_w	water saturation
S_{wirr}	irreductible water saturation
β_h	modelled amplitude damping of hydraulic transfer
β'_h	observed hydraulic amplitude damping
β_{th}	modelled amplitude damping of thermal transfer
β'_{th}	observed thermal amplitude damping
τ	period of the signal
ϕ	porosity (%)
θ	volumetric water content (%)
σ_{dc}	low frequency conductivity (S m^{-1})
λ	a fit parameter
ϖ	angular frequency (s^{-1})
ε_o	free-space permittivity ($\approx (36\pi)^{-1}\ 10^{-9}$ F m^{-1})
j	$(-1)^{1/2}$

1. Introduction

Many agricultural, environmental and engineering practices require the knowledge of the saturated hydraulic conductivity of the vadose zone. This knowledge is required, for example, in the design of agricultural drainage systems to lower seasonally high water tables and in the determination of the mounting of the water table under retention ponds or drainage areas of septic systems. The study of the temporal and spatial evolution of the water content and the thermal signal in porous materials as rainwater passes through the vadose zone is of scientific interest [3,18]. In fact, the water flow and contaminant transport through the vadose zone show an increased attention, for instance in waste disposal in porous medium, for the retention of pollutants within the pore space of rock masses in the near surface. It is also important in characterizing and predicting hydrological processes in the unsaturated zone.

On the other hand, many authors use temperature monitoring in order to evaluate the recharge in unsaturated soils [6,15,16]. Vertical water seepage in the vadose zone results in a convective heat transport that modifies the temperature profile and its variations with time. These authors have obtained some results using the temperature measurements in the determination of the vertical water seepage.

The purpose of this paper is to report on an experimental study of the volumetric water content evolution and the thermal transfer conducted over three hydrological cycles between August 2001 and November 2004 in an abandoned underground quarry (Saint-Germain-La-Rivière, France) located in a carbonate vadose zone. Then, a flow and heat transfer model was built, using the hydraulic and thermal properties of the carbonate vadose zone and their sinusoidal fluctuations, and its results were compared with experimental data obtained in situ.

2. Hydrological setting

The site is an underground quarry exploited by the ‘‘rooms and pillars’’ method. The cross-sections of

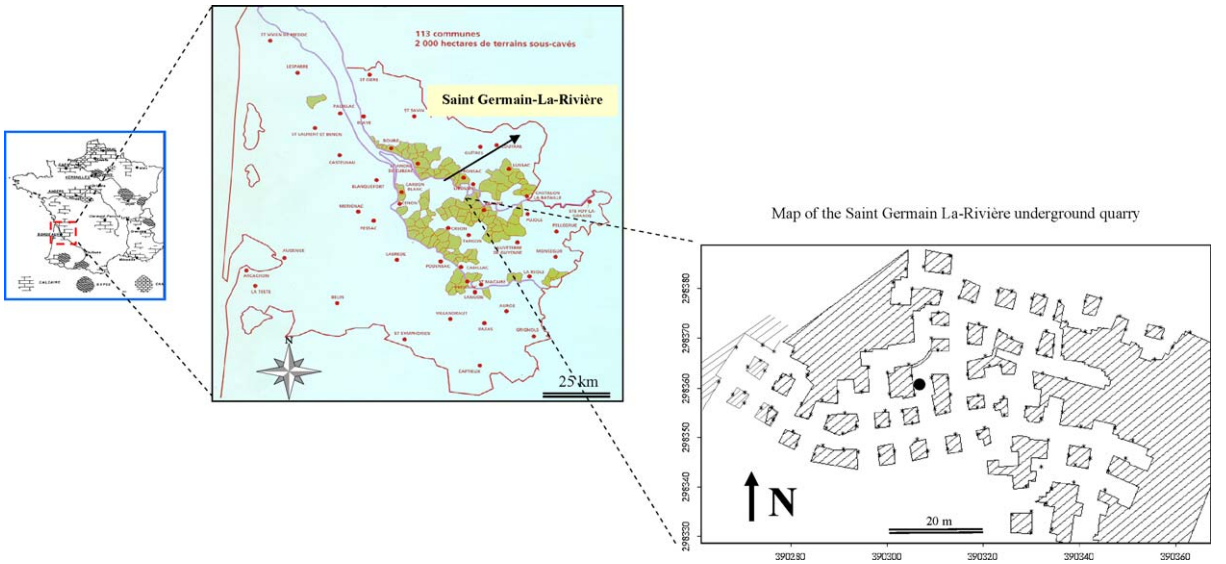

Fig. 1. Location of the underground quarry; location of time domain reflectometry (TDR) measurement points (*) of water content and temperature (●) inside the Saint-Germain-La-Rivière underground quarry.

Fig. 1. Localisation de la carrière souterraine étudiée ; localisation des points de mesure de teneur en eau par réflectométrie en domaine temporel (TDR) (*) et de température (●) à l'intérieur de la carrière souterraine de Saint-Germain-La-Rivière.

pillars vary from 6.6 m^2 to 69.9 m^2 (Fig. 1). Their height varies from 2.1 m to 4.4 m. These quarries have an overlying rock thickness of 3 to 7.2 m with a static stress ranging between 0.2 and 0.5 MPa. The experiments were focused on the spatial distribution and evolution with time and depth of the water content and temperature in the limestone of the quarry. The effective rainfall (P_{eff}) was considered to be the source of water in

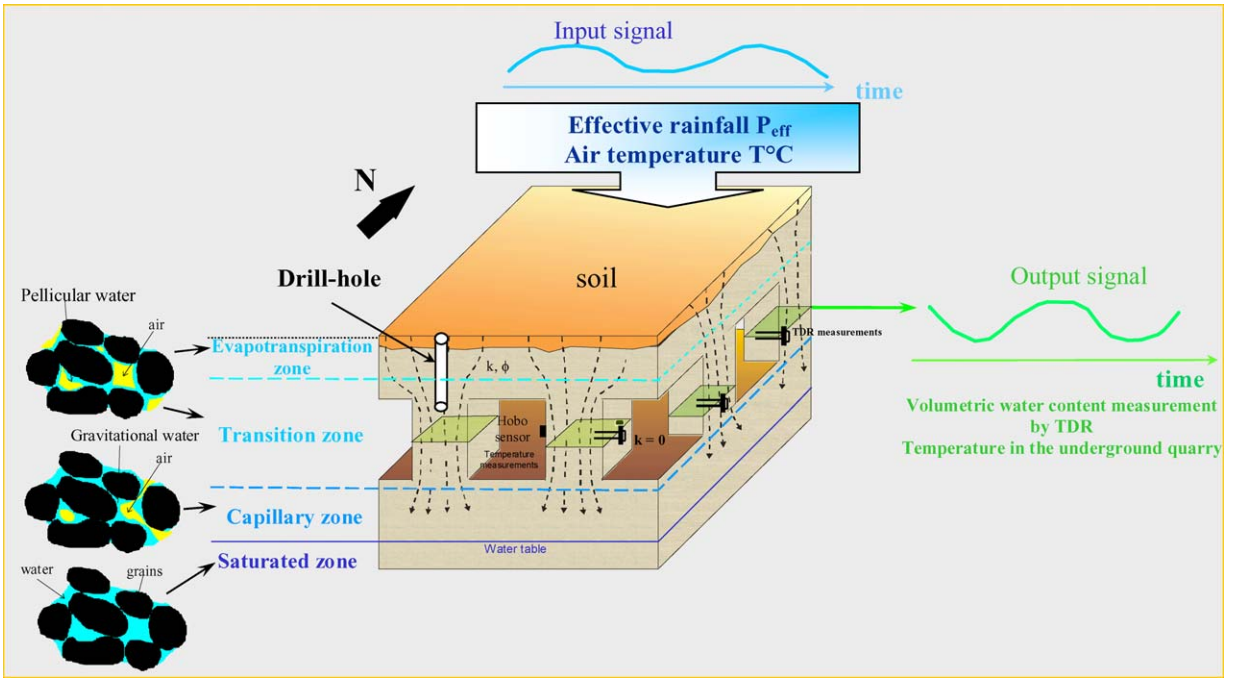

Fig. 2. Location of the underground quarry in the hydrological system (vadose zone) and methods of study.

Fig. 2. Localisation de la carrière souterraine étudiée dans le système hydrologique (zone vadose) et les méthodes d'étude.

the vadose zone and was used as the entrance signal of the system. The effective rainfall is defined as the difference between the precipitation water (P) and the real evapotranspiration (ET_r) $P_{eff} = P - ET_r$ (Fig. 2 and 3). The local topography is essentially flat and horizontal. Hence, runoff is not taken into account. The water flows mainly from the surface to the underlying aquifer through the porous pillars (Fig. 2).

The weather data are obtained from a meteorological *Météo France* station (Saint-Gervais). The real evapotranspiration is given by the Penman-Monteith model. Temperatures outside the quarry are taken from the meteorological station. A monthly time step is used in this study and is adequate for the characterization of the hydrological cycle (Fig. 3 and 4).

The porous network is represented by the matrix pores only as the fractures are sealed with impermeable red clays. More than 98 core samples have been taken from the pillars as well as from boreholes drilled from the surface through the rock cover immediately above the mine pillars in order to analyse the physical properties (Fig. 2).

In Saint-Germain-La-Rivière, the water table lies at 16 m below ground. The capillary rise is neglected at the studied scale. The average temperature in the underground quarry is $13 \pm 2\ ^{\circ}C$. This temperature varies during three hydrological cycles. The variation of temperature can play an important role in the exchange of water between the rock and the atmosphere of the quarry. The experiments performed in an underground limestone quarry in Vincennes (France) [9,11] show that for a temperature variation of about $2\ ^{\circ}C$, the saturation variation will be about 2% for a limestone whose average saturation is about 80%. In our case, the relative saturation variation is limited to about 1% for a limestone whose relative saturation varies between 35% and 50%. The exchange between the rock and the atmosphere is neglected at the studied scale. The water flow is mainly vertical, from the surface to the aquifer water table through the porous pillars.

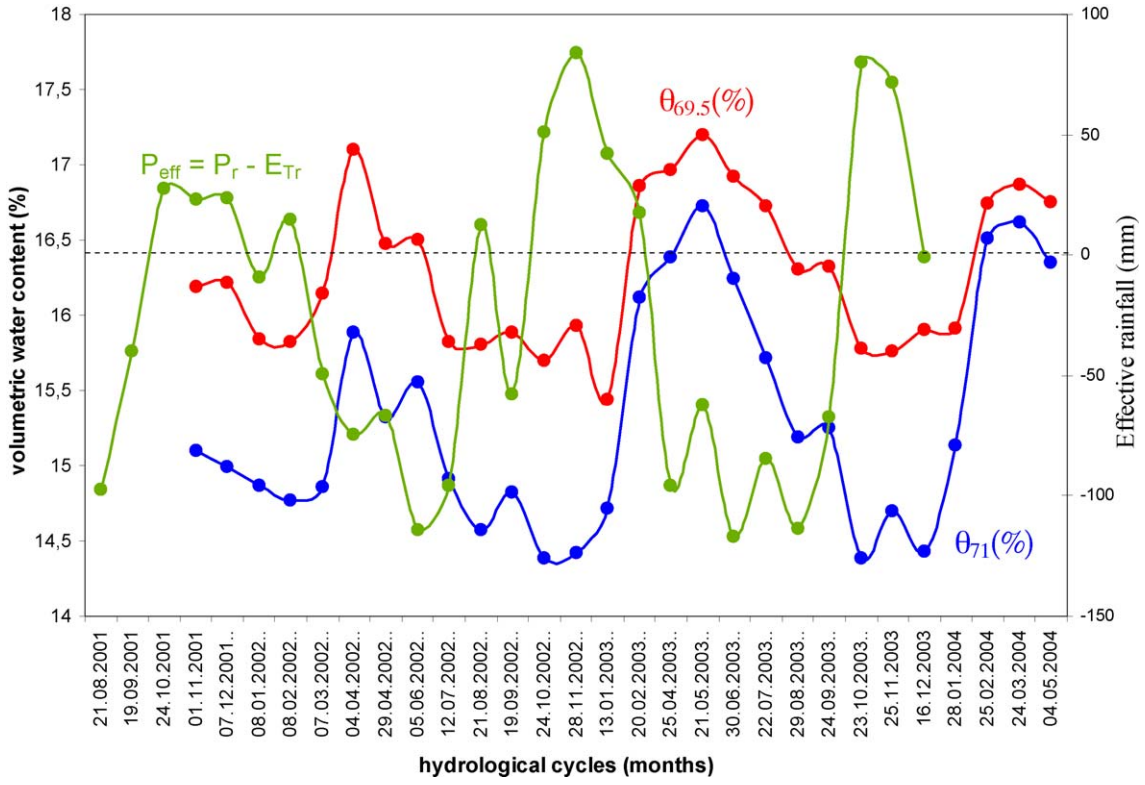

Fig. 3. Time series of time domain reflectometry (TDR) volumetric water content measurements at the 69.5 m and 71 m (NGF) depth in Saint-Germain-La-Rivière underground quarry during 2001–2004. Comparison between volumetric water content and effective rainfall during the same period.

Fig. 3. Séries temps des teneurs en eau par réflectométrie en domaine temporel (TDR) aux profondeurs de 69,5 m et de 71 m (NGF) dans la carrière souterraine de Saint-Germain-La-Rivière, durant la période 2001–2004. Comparaison entre la teneur en eau et les précipitations efficaces durant la même période.

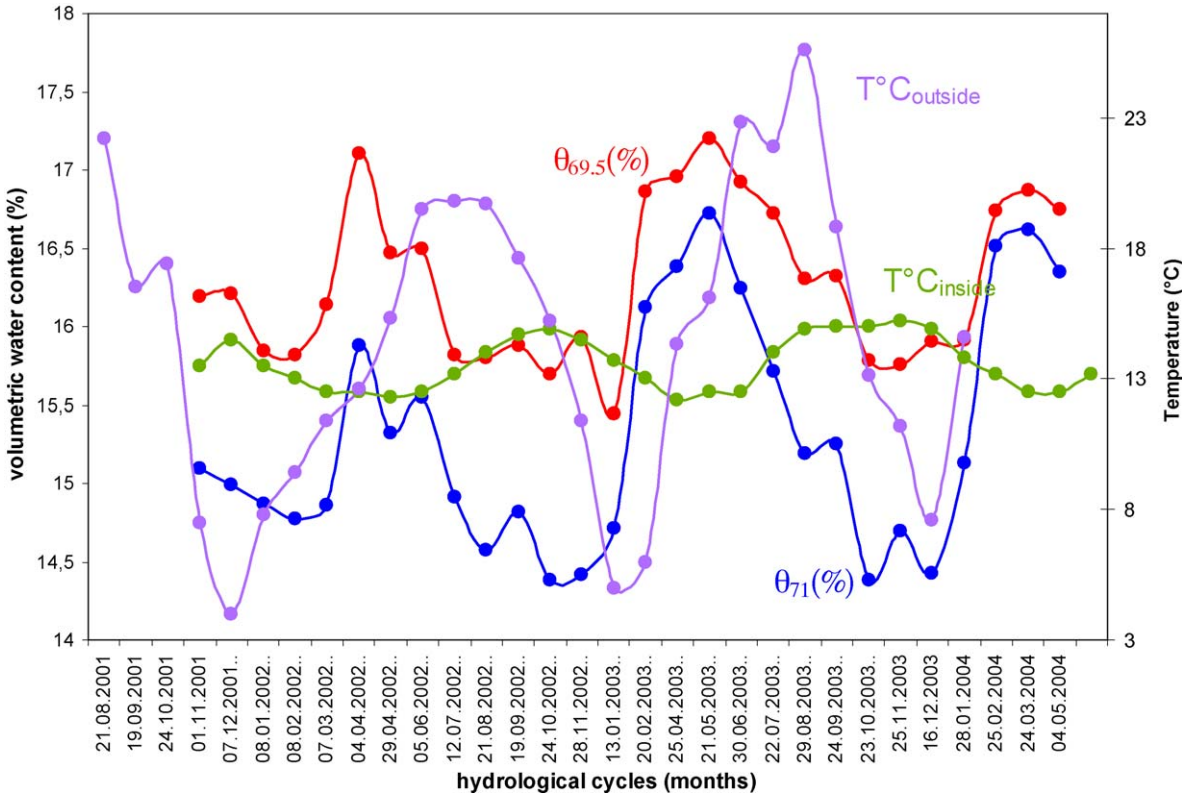

Fig. 4. Time series of the outside temperature, of the inside quarry temperature and of the time domain reflectometry (TDR) water content measurements at the 69.5 m and 71 m NGF depth in Saint-Germain-La-Rivière.

Fig. 4. Séries temps de la température à l'extérieur, de la température à l'intérieur de la carrière souterraine et des mesures de teneur en eau par réflectométrie en domaine temporel (TDR), aux profondeurs de 69,5 m et de 71 m dans la carrière de Saint-Germain-La-Rivière.

3. Methods and theoretical background

The method used to measure the soil-moisture content is the time domain reflectometry (TDR). Several authors [9,13,17] applied the TDR to the measurement of the apparent dielectric constant of soils, which is strongly dependent on their water content. The dielectric constant of a material is a complex quantity having the following form [7,8]:

$$K* = K' - j\left\{K'' + \left(\frac{\sigma_{dc}}{\omega\varepsilon_o}\right)\right\} \quad (1)$$

where: K* : the complex dielectric constant, Ḱ : the real part of the dielectric constant, Ḱ : the imaginary part of the dielectric constant or the electric loss, σ_{dc} : the low frequency conductivity (S m^{-1}), ϖ : the angular frequency (s^{-1}), ε_o : the free-space permittivity ($\approx (36\pi)^{-1} \times 10^{-9}$ F m^{-1}), j : $(-1)^{1/2}$.

Different variables, such as texture, structure, soluble salts, water content, temperature, density, and measurement frequency affect the dielectric constant of soils [17]. For frequencies between 1 MHz and 1 GHz, the real part of the dielectric constant does not appear to be strongly dependent on the frequency. The TDR-method is based on a measuring the transit time of an electromagnetic wave in a transmission line of a known length within the material sample:

$$C \approx \frac{C_o}{\sqrt{K'}} \quad (2)$$

where C_o is the velocity of light (3×10^8 m s^{-1}).

The wave travels along two rods of the TDR-probe of length l, it is reflected at the end of the rods and travels back the same way. The velocity measurement is transformed into a transit time measurement following the relationship (C = 2l/t) from which one gets:

$$K' = \left(\frac{tC_o}{2l}\right)^2 \quad (3)$$

In a porous medium, made of at least three components, air (K′ = 1), grains (K′ = 3 to 5) and water

($K' = 81$), the velocity depends both on the proportions of these components and on the nature of the grains.

Different models have been proposed to describe the relationship between the volumetric water content θ and the relative dielectric constant K'. Topp et al. [17] showed that a third-order polynomial function was adequate to describe the relationship between K' and θ as:

$$\theta = D + CK' + BK'^2 + AK'^3 \quad (4)$$

where $A = 4.3 \times 10^{-6}$, $B = -5.5 \times 10^{-4}$, $C = 2.92 \times 10^{-2}$, $D = -5.3 \times 10^{-2}$.

Although the individual calibration for each soil/rock may be necessary to obtain precise measurements of water content, this empirical relationship is still the most widely used in soil science.

The volumetric water content (θ) equals the product of porosity (θ) and water saturation (S_w). In a water-saturated rock, the water content is a measurement of porosity: $\theta = \theta S_w$.

4. Experimental results

4.1. Water content measurements

Three hydrological cycles (August 2001 to November 2004) were studied.

A monthly analysis of volumetric water content measurements and effective rainfall indicated that the rock saturation at the studied site varied between 35% and 50% (Table 1). Throughout the three cycles, the saturation never reached 100%. The maximum saturations were observed during cycle 2 (January 2003 to January 2004) (saturation ≈ 50.6%) while the minimum saturation observed was 35.1% (Table 1).

The volumetric water content of the vadose zone shows maxima and three minimum values (Fig. 5):

- **first cycle (January 2002 to January 2003):** the volumetric water content in the vadose zone at 69.5 m (NGF) reached a maximum of 17.1% during April 2002 (water saturation ≈ 50.3%). This maximum was related to the maximum effective rainfall of October 2001 ($P_{eff} \approx 27.6$ mm). There was a six month time-lag between the rainfall events of October 2001 and their inference at depths of 5.85 m and 7.35 m. The rates of decrease (T_a) and increase (T_r) in saturation of the carbonate formation in the vadose zone of 5.85 and 7.35 m are given in Table 2;
- **second cycle (January 2003 to January 2004):** the volumetric water content in the vadose zone at 69.5 m (NGF) reached a maximum of 17.2% in May 2003

Table 1
Volumetric water content and water saturation measured during three hydrological cycles in the underground quarry.
Tableau 1
Teneurs volumiques en eau et saturations mesurées durant les trois cycles hydrologiques dans la carrière souterraine.

Site	Cote m NGF	Depth Δz (m)	ϕ	Cycle 1: January 2002 to January 2003				Cycle 2: January 2003 to January 2004				Cycle 3: January 2004 to May 2005			
				Volumetric content (%)		Saturation (%)		Volumetric content (%)		Saturation (%)		Volumetric content (%)		Saturation (%)	
				Minimum	Maximum	Minimum	Maximum	Minimum	Maximum	Minimum	Maximum	Minimum	Maximum	Minimum	Maximum
Saint-Germain 1	69.5	7.35	0.34	15.44	17.1	45.4	50.3	15.76	17.2	46.3	50.6	15.76	16.87	46.3	49.6
Saint Germain 2	71	5.85	0.41	14.38	15.88	35.1	38.7	14.38	16.72	35.1	40.7	14.38	16.62	35.1	40.5

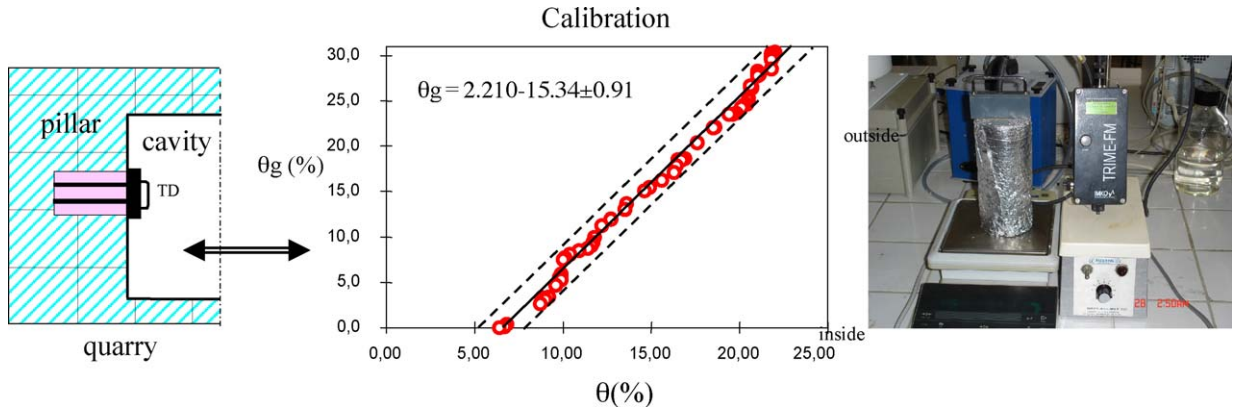

Fig. 5. Calibration process: the water content θ_g is measured by direct weighing of the sample and by the value θ given by the TDR technique.

Fig. 5. Calibration : la teneur en eau θ_g mesurée par pesée de l'échantillon et par la technique de réflectométrie en domaine temporel (TDR) (θ).

Table 2
Water desaturation rate (T_a) and water saturation rate (T_r) (in % days^{-1}) in the vadose zone.
Tableau 2
Taux de désaturation en eau (T_a) et taux de saturation en eau (T_r) (en % jour^{-1}) dans la zone vadose.

	Cycle 1	Cycle 2 Saint Germain-La-Rivière 7.35 m depth (69.5 m NGF)	Cycle 3	Cycle 1	Cycle 2 Saint Germain-La-Rivière 5.85 m depth (71 m NGF)	Cycle 3
$Tr = \frac{\Delta\theta}{\Delta t}(\%\,\mathrm{day}^{-1})$	0.0058	0.00766	–	0.0073	0.0151	–
$T_a = \frac{\Delta\theta}{\Delta t}(\%\,\mathrm{day}^{-1})$	0.0223	0.01375	0.0093	0.0202	0.01125	0.0147

(water saturation ≈ 50.6%). This maximum was related to the maximum effective rainfall of October 2002 (P_{eff} ≈ 84 mm), also with a six-month time-lag. The desaturation (T_a) and saturation rates (T_r) of the carbonate formation in the vadose zone are $T_a = 0.00766\%\ \mathrm{day}^{-1}$ and $T_r = 0.01375\%\ \mathrm{day}^{-1}$ at 5.85 m depth. The rates of decrease (T_a) and increase (T_r) in saturation at depths of 5.85 and 7.35 m are given in Table 2;

- **third cycle (January 2004 to May 2004):** the volumetric water content of the vadose zone at 69.5 m (NGF) reached a maximum of 16.9% in March 2004 (water saturation ≈ 49.6%). This maximum was related to the maximum effective rainfall of October 2003 (P_{eff} ≈ 79.8 mm), again with a six-month time-lag. The rates of decrease (T_a) and increase (T_r) in saturation at depths of 5.85 and 7.35 m are given in Table 2.

4.2. Thermal transfers

The temperatures in the quarry are measured with a Hobo apparatus located in its centre (Fig. 4). Mean monthly values are obtained from hourly measurements for comparison with other monthly measurements (for example the water saturation).

We also observed three thermal cycles related to three maximum and three minimum values of the temperature outside and inside the quarry.

The thermal signal outside the quarry is characterized by maximum and minimum average temperature values (Fig. 4). The thermal signal evolution inside the quarry is characterized by maximum and minimum average temperature values (Fig. 4). There is a 3.5-month time-lag between the thermal signal outside the quarry and its inference at the 5.85 m depth.

4.3. Laboratory measurements

4.3.1. Calibration of the time domain reflectometry and representativity

The calibration process aims at obtaining the true value of the water content from the in situ TDR measurements. The TDR measurements require the probe to be in good contact with the rock. A slight void space between the electrode and the material causes significant measurement errors because the estimated K′ is sensitive to the dielectric properties of the medium. Some authors [2] have quantified the effect of the gaps around the electrodes analytically and numerically. They showed that air-filled gaps caused a significant

underestimation of K′, whereas water-filled gaps result only in a slight overestimation of K′.

In a TDR probe with two rods, the main energy of the electromagnetic waves is restricted to a cylinder with a diameter equal to twice the distance between the two rods (Fig. 5) [8,10,13]. Hence, the rock sample measurement volume is a cylinder of approximately 8 cm in diameter and 16 cm in length. The calibration uses the volumetric water content obtained by the TDR and the gravimetric one obtained by the direct weighing of the sample. For the calibration of the TDR apparatus, we used a core sample whose size was of the order of the rock volume measured by the electromagnetic field (8 cm in diameter and 16 cm in length). The core is first dried with a primary vacuum and then in a drying oven at 60 °C. Next, the core is vacuum-saturated with water flushed at a high velocity to ensure good saturation. The core is progressively unsaturated at ambient temperature. The water content θ_g is measured by direct weighing of the sample and by the value θ given by the TDR technique. From these, we obtain the following calibration relationship (Fig. 5):

$$\theta_g = 2.21\theta - 15.34 \pm 0.91 \quad (5)$$

The discrepancy between the TDR volumetric water content and the gravimetric one is due to the quality of the contact between TDR probes and the porous rock.

The spatial representativity of the measurements is verified by comparing the experimental distribution DM_{obs} to the punctual distribution DM_{al} predicted by Poisson's law with the same density. From this, we obtain the coefficient R of spatial representativity [7]:

$$R = \frac{DM_{obs}}{DM_{al}} = \frac{2\sqrt{n}\sum_{i=1}^{n} Dobs_i}{n\sqrt{S}} \quad (6)$$

where n is the number of the TDR measurements, S is the area of the studied quarry (in m^2), i varies from 1 to n, with $Dobs_i$ the length between a point i and its nearest neighbour (in m). If the coefficient R ranges between 0.9 and 2.4, the number of measurement points is representative. Table 3 gives the values of coefficient R obtained at different levels of the quarry. The values of R vary between 1.23 and 1.26. So, for each quarry, the number of TDR measurement points is sufficient. Following this verification, the image mode of Geographic Information Systems (GIS) was used for the spatial analysis and map of different selected measurements.

Table 3
Values of the data spatial representativity coefficient R.
Tableau 3
Valeurs du coefficient de représentativité spatiale des données R.

Sites	Depth Δz (m)	Number of measurements	Area (m^2)	R
Saint-Germain 1	5.85	145	3369	1.26
Saint-Germian 2	7.35	140	3369	1.23

4.3.2. Hydraulic properties

The basic physical properties used in this model are the permeability and porosity. Their measurement was obtained from 98 cylindrical samples. The air permeability of the rock was determined by flow experiments using an IFP49 variable head air permeameter, and converted into hydraulic conductivity k. In the case of linear beds in series, the appropriate average hydraulic conductivity is equal to the harmonic mean as:

$$k = \frac{L}{\Sigma}\left\{\frac{L_i}{k_i}\right\}$$

where L_i is the thickness of each bed and k_i is the measured hydraulic conductivity of each bed.

The porosity was obtained by mercury injection. The average porosity ϕ takes into account the porosity of all beds. In the case of two-phase flow (water and air), the hydraulic diffusivity is defined by:

$$D_h = \frac{k_{eff}}{\phi} = \frac{k_{rw}k}{\phi} \quad (7)$$

where k_{eff} is the effective hydraulic conductivity; k_{rw} is the relative water permeability; k is the saturated hydraulic conductivity.

The relative water permeability is generally assumed to depend only on the water saturation S_w and ranges between 0 and 1. We used the Brooks-Corey pressure–saturation curves [1]:

$$S_e = \frac{S_w - S_{wirr}}{1 - S_{wirr}} = \left(\frac{P_c}{P_b}\right)^{-\lambda} \quad (8)$$

where P_b is the bubbling pressure, λ is a fit parameter, S_e is the normalized saturation, S_{wirr} the irreducible water saturation; P_c is the capillary pressure.

For the drainage case and for the wetting phase, the water relative permeability can be estimated by the empirical Brooks-Corey model [1]:

$$k_{rw}(S_w) = \left(\frac{S_w - S_{wirr}}{1 - S_{wirr}}\right)^{\left(2+2.5\lambda\right)/\lambda} \quad (9)$$

Many authors propose a Corey-type water relative permeability:

$$k_{rw}(S_w) = \left(\frac{S_w - S_{wirr}}{1 - S_{wirr}}\right)^{3+2/\lambda} \quad \text{or } k_{rw} = S_w^5 \quad (10)$$

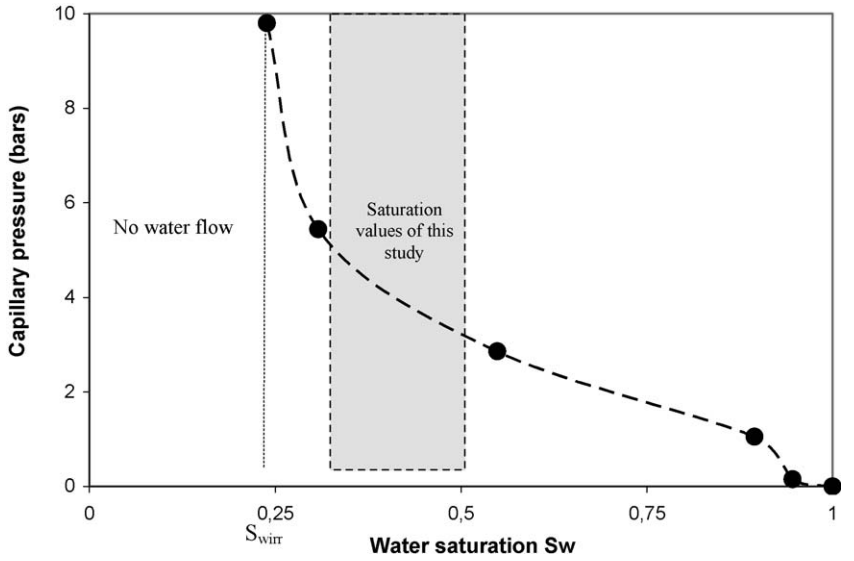

Fig. 6. Experimental curve of air-water capillary pressure P_c versus water saturation S_w.

Fig. 6. Courbe expérimentale de pression capillaire air-eau P_c en fonction de la saturation en eau S_w.

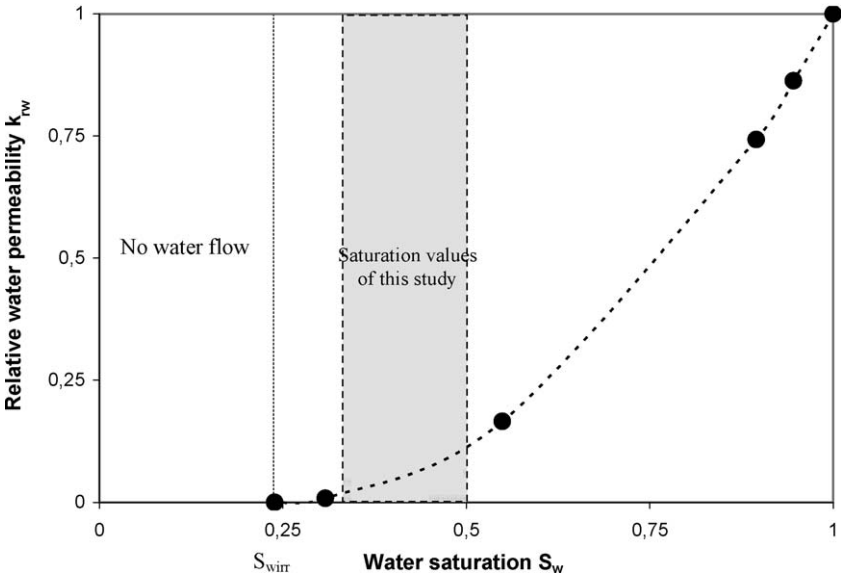

Fig. 7. Water relative permeability k_{rw} versus water saturation S_w obtained by the Corey-type model (equation (19)).

Fig. 7. Perméabilité relative à eau k_{rw} en fonction de la saturation S_w obtenue avec le modèle de type Corey (Éq. (19)).

In this paper, we used the simple relation given by [1]:

$$k_{rw}(S_w) = \left(\frac{S_w - S_{wirr}}{1 - S_{wirr}}\right)^{\alpha} \quad (11)$$

with $\alpha = 2$, for $S_w > 0.25$ and $k_{rw} = 0$ for $S_w < 0.25$.

Fig. 6 gives the experimental curve of the water-air capillary pressure versus the water saturation obtained by the ''porous plate'' method [5]. In our case, the experimental irreducible water saturation is $S_{wirr} = 0.25$. From equation (11) and using this experimental curve of Fig. 6, we obtained the relationship between the water relative permeability and the water saturation (Fig. 7). Table 4 gives different petrophysical properties at different depth used in this study during the modelling process.

Table 4
Hydraulic properties measured on the studied site and used for modelling water transfer.
Tableau 4
Propriétés hydrauliques mesurées dans le site d'étude et utilisées dans le modèle de transfert hydrique.

Sites	Cote m NGF	Depth Δz (m)	ϕ	k 10^{-6} (m s^{-1})	k_{rw} minimum	Maximum	k_{eff} 10^{-6} (m s^{-1})		D_h 10^{-6} (m s^{-1})	
							Minimum	Maximum	Minimum	Maximum
Saint-Germain 1	69.5	7.35	0.34	4.5	0.049	0.123	0.221	0.554	0.65	1.63
Saint-Germain 2	71	5.85	0.41	4.5	0.022	0.056	0.099	0.252	0.241	0.614

4.3.3. Thermal properties

In order to evaluate the thermal transfer in the carbonate vadose zone, we define different thermal properties which depend on several time-independent variables. Many authors have studied the changes of thermal properties with moisture content changes [6,14–16]. The thermal diffusivity D_{th} (m^2 s^{-1}) in an unsaturated medium is defined by:

$$D_{th} = \frac{k_n}{C_v} \tag{12}$$

C_v is the volumetric heat capacity:

$$C_v = C_w\theta + C_s(1-\phi) \tag{13}$$

where C_s is the volumetric heat capacity of the solid fraction ($\approx 2 \times 10^6$ J m^{-3} K^{-1}); C_w is volumetric heat capacity of water (4.18×10^6 J m^{-3} K^{-1}); ϕ is the porosity; θ is the volumetric water content.

k_n the thermal conductivity is estimated by:

$$k_n = (0.8908 - 1.0959\phi)k_s + (1.2236 - 0.3485\phi)\theta \tag{14}$$

where k_s is the thermal conductivity of the limestone (2.1–3.4 W m^{-1} K^{-1}).

Equations (12)–(14) allow us to obtain maximum and minimum values of the thermal diffusivity (0.59–0.61 $\times 10^{-6}$ m^2 s^{-1}) using a uniform porosity ϕ = 41%, a maximum volumetric water content θ = 16.7%, a minimum volumetric water content θ = 14.4%, a volumetric heat capacity of the solid fraction $C_s \approx 2 \times 10^6$ J m^{-3} K^{-1}, a volumetric heat capacity of water $C_w = 4.18 \times 10^6$ J m^{-3} K^{-1} and a thermal conductivity of the limestone k_s = 2.1–3.4 W m^{-1} K^{-1}.

5. Modelling and discussions

5.1. Propagation, amplitude damping and phase lag of hydraulic/thermal signal – Model used in this study

In this study, we use the same model to analyse the phase lag and the amplitude damping of the thermal signal and volumetric water content at different depths in a homogeneous porous medium. If the thermal signal or volumetric water content signal at depth $z = 0$ (air temperature outside the cavity, effective rainfall) is a sinusoidal signal with a period τ, the thermal signal or volumetric water content measured at depth z must be again a sinusoidal signal with the same period τ but with a phase lag and damped. If we take into account only the conduction or diffusion process, a thermal or hydraulic signal at z = 0 defined by [4,12]:

$$T(t,0) = A(0)\sin\left(\frac{2\pi t}{\tau}\right) \tag{15}$$

becomes at depth $z = -|z|$:

$$T(t,z) = A(0)e^{\sqrt{\pi/\tau D}z}\sin\left(\frac{2\pi t}{\tau} - \sqrt{\frac{\pi}{\tau D}}z\right) \tag{16}$$

where D is the diffusivity of the porous medium; t is time; A(0) is the amplitude of the input signal. From equation (16) we can deduce the amplitude of hydraulic and thermal signals at depth |z|:

$$A(z) = A(0)e^{-\sqrt{\pi/\tau D}\}|z|} \tag{17}$$

The amplitude damping of the signal can be written:

$$\beta = \ln\frac{A(z_2)}{A(z_1)} = \sqrt{\frac{\pi}{\tau D}}|z_2 - z_1| \tag{18}$$

From equation (16) we can deduce the time t for the hydraulic and thermal signals to pass from depth z_1 to z_2:

$$t = \sqrt{\frac{\tau}{4\pi D}}|z_2 - z_1| \tag{19}$$

In the case of hydraulic transfer, D becomes D_h and equations (18) and (19) can be rewritten:

$$\beta_h = \ln\frac{A(z_2)}{A(z_1)} = \sqrt{\frac{\pi}{\tau D_h}}||z_2 - z_1 = \sqrt{\frac{\pi\phi}{\tau(S_w - 0.25/1 - 0.25)^2 k}}|z_2 - z_1| \tag{20}$$

$$t_h = \sqrt{\frac{\tau}{4\pi D_h}}|z_2 - z_1| = \sqrt{\frac{\tau\phi}{4\pi k_{eff}}}|z_2 - z_1|$$
$$= \sqrt{\frac{\tau\phi}{4\pi k_{rw} k}}|z_2 - z_1|$$
$$= \sqrt{\frac{\tau\phi}{4\pi (S_w - 0.25/1 - 0.25)^2 k}}|z_2 - z_1| \quad (21)$$

In the case of thermal transfer D becomes D_{th} and equations (20) and (21) can be rewritten:

$$\beta_{th} = \ln\frac{A(z_2)}{A(z_1)} = \sqrt{\frac{\pi}{\tau D_{th}}}|z_2 - z_1| = \sqrt{\frac{\pi c_v}{\tau k_n}}|z_2 - z_1| \quad (22)$$

$$t_{th} = \sqrt{\frac{\tau}{4\pi D_{th}}}|z_2 - z_1| = \sqrt{\frac{\tau c_v}{4\pi k_n}}|z_2 - z_1| \quad (23)$$

5.2. Results of the modelling

Table 5 gives the modelling results of the water transfer time in the vadose zone. The comparison between the predicted time and the measured time from TDR measurements generally shows a good agreement. The favourable modelling results show that the hydraulic transfer is dominated by the physical properties of the porous medium and its depth. The convection (which is neglected in the model) thus plays a minor role in the hydraulic transfer through the vadose zone. The discrepancy between the predicted hydraulic transfer time t_h and the measured hydraulic transfer time t_h' is mainly due to the fact that the model does not take into account convection.

This study shows that it is not possible to neglect the transfer of water through the unsaturated zone in a carbonate environment such as our site. This is an important point when predicting recharge to an aquifer. Some approaches of the hydraulic transfer in an unsaturated zone have been based on the assumptions that the hydraulic transfer is instantaneous. This study shows that the transfer time is not instantaneous and can be of the order of 6 months for a depth of 5–7 m in a limestone of saturated hydraulic conductivity of 4.5×10^{-6} m s^{-1}.

Table 6 gives the comparison between the amplitude damping of the hydraulic signal at two different depths z_1 and z_2 obtained by modelling (equation (20)) and measured with the TDR technique. We observe a good agreement between modelling results and experimental data. From this, we deduce that above the water table the hydraulic signal amplitude must be near zero and the water content must be constant.

Table 7 gives the modelling results of the thermal transfer time. The comparison between the predicted time values obtained from equation (23) and the measured time shows a discrepancy: the transfer time of the predicted thermal transfer (4.6–4.7 months) is longer than the measured value (3.5 months). The difference is likely due to an air circulation between

Table 5
Comparison between the predicted time of water transfer (t_h) from equation (21) and the measured time of water transfer (t_h').
Tableau 5
Comparaison entre le déphasage du signal hydrique (t_h) prédit par l'équqtion (21) et celui du signal hydrique mesuré (t_h').

Sites	Depth Δz (m) Δz	D_h 10^{-6} (m s^{-1}) Minimum	Maximum	t_h 10^6 (s) Maximum	Minimum	t_h (months) Maximum	Minimum	t_h' 10^6 (s)	t_h' (months)
Saint-Germain 1	5.85	0.241	0.614	18.9	11.8	7.2	4.5	15.6	6
Saint-Germain 2	7.35	0.65	1.63	14.4	9.12	5.5	3.5	15.6	6

$D_h = k_{eff}/\phi$: hydraulic diffusivity.

Table 6
Comparison between the predicted amplitude damping (β_h) of water transfer from equation (20) and measured damping (β_h') determined from the TDR measurements.
Tableau 6
Comparaison entre l'atténuation du signal hydrique (β_h) prédite par l'Éq. (20) et celle mesurée (β_h') du signal hydrique obtenu par la méthode TDR.

Sites	Depth (m) Δz	τ 10^6 (s)	D_h 10^{-6} (m s^{-1}) Minimum	Maximum	β_h Maximum	Minimum	β_h' $A(Z_2)/A(Z_1)$
Saint-Germain	1.5	31.56	0.65	1.63	0.6	0.4	0.5

τ: period of the sinusoidal signal; $D_h = k_{eff}/\phi$: hydraulic diffusivity.

Table 7
Comparison between the predicted time of thermal transfers (t_{th}) from equation (23) and that measured (t'_{th}) in underground quarry.
Tableau 7
Comparaison entre le déphasage du signal thermique (t_{th}) prédit par l'Éq. (23) et celui mesuré-t_h' dans la carrière souterraine.

Sites	Depth (m)	D_{th} 10^{-6} (m^2 s^{-1})		τ 10^6 (s)	t_{th} (months)		t'_t (months)
	Δz	Maximum	Minimum		Minimum	Maximum	
Saint-Germain 1	5.85	0.61	0.59	31.56	4.5	4.6	3.5

D_{th}: thermal diffusivity.

Table 8
Comparison between the predicted amplitude damping (β_{th}) of thermal signal from equation (22) and that measured (β'_{th}) in the underground quarry.
Tableau 8
Comparaison entre l'atténuation du signal thermique (β_{th}) prédite par l'Éq. (22) et celle mesurée (β'_{th}) dans la carrière souterraine.

Sites	Depth (m)	τ 10^6 (s)	D_{th} 10^{-6} (m^2 s^{-1})		β_{th}		β'_{th} $A(Z_2)/A(Z_1)$
	Δz		Maximum	Minimum	Minimum	Maximum	
Saint-Germain 1	5.85	31.56	0.61	0.59	2.3	2.4	1.9

τ: period of the sinusoidal signal; D_{th}: thermal diffusivity.

outside (atmosphere) and inside the quarry and a rapid re-equilibration of air temperature in the vadose zone. The model used does not take into account the dynamics of the air in the quarry. The second observation is that the measured water transfer times in the vadose zone (about 6 months) are longer than the measured thermal transfer (3.5 months). On the contrary, the predicted water transfer time in the vadose zone (4.5–7 months) is equal to the predicted thermal transfer time (4.5–4.6) (Tables 5 and 7). The good agreement between the predicted temperature variation versus time and the predicted water transfer time is consistent with the results of many authors such as Cheviron et al. [6], Tabbagh et al. [15]. In fact, the time variation of the temperature in an unsaturated medium can be used for the determination of the vertical water flow rate.

Table 8 gives the comparison between the amplitude damping of the thermal signal at two different depths z_1 and z_2 obtained from by modelling β_{th} (equation (22)) and measured β_{th}' from the TDR measurements. The discrepancy between the predicted amplitude damping (2.3–2.4) and the measured amplitude damping (1.9) is likely due to the influence of the air circulation in the quarry.

6. Conclusions

This paper studied the water and heat transfer in the vadose zone of a carbonate formation during three hydrological cycles (August 2001–May 2004). The application of the TDR method to determine the water content of the porous rock was used to monitor the water transfer. More than 285 measurements of rock water content during three hydrological cycles distributed throughout the quarry show a permanently undersaturated limestone (between 35% and 50%). Three periods of maximum water content correspond to three effective rainfall maxima but with a time-lag. The results showed that the time for water transfer was long, about 6 months. The phase lag and amplitude damping of the hydraulic and thermal signal with depth have been modelled taking into account the measured physical properties of the porous medium. The comparison between the predicted and measured hydraulic transfer time is good; however, the comparison between the predicted and measured thermal transfer time shows a discrepancy, most likely due to air circulation between the outside (atmosphere) and inside of the quarry and a rapid re-equilibration of the temperature in the vadose zone with that of the air. The predicted water transfer time in the vadose zone (4.5–7 months) is equal to the predicted thermal transfer time (4.5–4.6). This good agreement is consistent with the results of many authors.

Acknowledgments

The authors thank Ghislain de Marsily for insightful reviews and input.

References

[1] P.M. Adler, J.V. Thovert, C. Jacquin, P. Morat, J.L. Le Mouël, Electrical signals induced by the atmospheric pressure variations in unsaturated media, C. R. Acad. Sci. Paris Ser. IIa. 324 (1997) 711–718.
[2] A.P. Annan, Time domain reflectometry—Air-gap problem for parallel wire transmission lines, Rep. Activ., Part B, Geol. Surv. of Canada, Ottawa, Ont., Canada. 77-1B (1977) 59–62.

[3] A. Binley, P. Winship, R. Middleton, M. Pokar, J. West, High-resolution characterization of vadose zone dynamics using cross-borehole radar, Water Resour. Res. 37 (2001) 2639–2652.
[4] A. Burger, E. Recordon, D. Bovet, L. Cotton, B. Saugy, Thermique des nappes souterraines, Presses Polytechniques Romandes, Paris, 199, 341 p.
[5] A. Cerepi, C. Loisy, R. Toullec, R. Burlot, S. Galaup, M. Schmutz, Electrical behaviour of saturated and unsaturated geological carbonate porous systems, Stud. Surf. Sci. Catal. 160 (2007) 713–719.
[6] B. Cheviron, R. Guérin, A. Tabbagh, H. Bendjoudi, Determining long-term recharge by vertical soil temperature profiles at meteorological stations, Water Resour. Res. 41 (9) (2005) 9501–9507.
[7] C. Collet, Systèmes d'information géographique en mode image (Presses Polytechniques et Universitaires Romandes, Lausanne), 1992.
[8] P. De Clerck, Mesure de l'humidité des sols par voie électromagnétique, Tech. Routière. 3 (1985) 6–15.
[9] H. Fellner-Feldegg, The measurement of dielectrics in time domain, J. Phys. Chem. 73 (1969) 616–623.
[10] J.P. Laurent, Profiling water content in soils by TDR: experimental comparison with the neutron probe technique (invited Lecture at the Consultants' meeting), AIEA, Vienna, 23–25 Nov. 1998.
[11] P. Morat, J.L. Le Mouël, Signaux électriques engendrés par des variations de contrainte dans des roches poreuses non saturées, C. R. Acad. Sci. Paris Ser. II. 315 (1992) 955–963.
[12] F. Perrier, P. Morat, Characterization of electrical daily variations induced by capillary flow in the non-saturated zone, Pure Appl. Geophys. 157 (2000) 785–810.
[13] S.R. Seshandri, Fundamentals of transmission lines and electromagnetic fields, Addison-Wesley, Reading, Mass, 1971.
[14] R. Stallman, Steady one dimensional fluid flow in a semi-infinite porous medium with sinusoidal surface temperature, J. Geophys. Res. 70 (1965) 2821–2827.
[15] A. Tabbagh, H. Bendjoudi, Y. Benderitter, Determination of recharge in unsaturated soils using temperature monitoring, Water Resour. Res. 35 (1999) 2439–2446.
[16] M. Taniguchi, Evaluation of vertical groundwater fluxes and thermal properties of aquifers based on transient temperature-depth profiles, Water Resour. Res. 29 (1993) 2021–2026.
[17] G.C. Topp, J.L. Davis, A.P. Annan, Electromagnetic determination of soil water content: measurements in coaxial transmission lines, Water Resour. Res. 16 (1980) 574–582.
[18] J. Walker, G.R. Willgoose, J.D. Kalma, The nerrigundah data set: soil moisture patterns, soil characteristics, and hydrological flux measurements, Water Resour. Res. 37 (2001) 2653–2658.